Priebe, J. B., Radnik, J., Kreyenschulte, C., Lennox, A. J. J., Junge, H., Beller, M., & Brückner, A. (2017). H_2 Generation with (Mixed) Plasmonic Cu/Au-TiO_2 Photocatalysts: Structure–Reactivity Relationships Assessed by in situ Spectroscopy. *ChemCatChem*, *9*(6), 1025-1031. https://doi.org/10.1002/cctc.201601361

H_2 generation with (mixed) plasmonic Cu,Au-TiO_2 photocatalysts: Structure-reactivity relationships assessed by in situ spectroscopy

Jacqueline B. Priebe,[a] Jörg Radnik,[b] Carsten Kreyenschulte,[a] Alastair J. J. Lennox,[c] Henrik Junge,[a] Matthias Beller,[a] and Angelika Brückner[a]*

Dedicated to Prof. Dr. Bernhard Lücke on the occasion of his 80th birthday

Abstract: Monometallic Cu- and bimetallic Cu/Au-TiO_2 catalysts were prepared by impregnation (IM) and reductive precipitation (RP) methods in sequential (SP) and simultaneous mode (CP) and tested for photocatalytic H_2 generation from H_2O/methanol mixtures with visible (400 – 700 nm) and UV-vis light (320 – 500 nm). Comprehensive studies by HR-STEM, XPS and different in situ methods (XANES, UV-vis and EPR spectroscopy) revealed that IM leads to dispersed surface Cu species with no clear particle formation being poorly active under visible light, while plasmonic Cu^0 nanoparticles formed by RP are about three times more active under the same conditions. In Cu/Au-TiO_2 catalysts prepared by RP-SP, highly dispersed Cu surface species boost especially H_2 production under UV-vis light, due to the effective separation within TiO_2 and electron trapping by Cu, while small Cu^0 and Au^0 particles remain widely separated. When Cu/Au-TiO_2 catalysts are prepared by RP-CP, mixed Cu-Au particles of uniform size (4-8 nm) provide the highest H_2 evolution rates under visible light, due to effective surface plasmon resonance absorption.

Introduction

Due to global warming and increasing concerns about the depletion of fossil resources, there is a growing need for the development of sustainable energy carriers such as H_2 from water. Photocatalytic water reduction using sunlight, which contains mainly visible radiation, would be an attractive and environmentally benign alternative to the still dominating H_2 production from fossil resources. However, up to now sufficiently effective photocatalysts making the "up-hill" water-splitting reaction economically feasible are still not available.[1] TiO_2 is one of the most investigated and promising semiconductor photocatalysts due to its high chemical and photochemical stability, abundance and non-toxicity.[2] However, UV light, comprising only about 4 % of the solar radiation, is needed to excite transitions of electrons from the valence band into the conduction band, from which they can reduce protons at the TiO_2 surface. With pristine TiO_2, fast recombination of separated electrons and holes usually leads to low quantum efficiencies. Therefore, the introduction of coinage metal nanoparticles (Au, Ag, Cu) is a promising route to overcome the limitations of TiO_2 based photocatalysts since these offer two important advantages for efficient photocatalytic performance: i) they form a Schottky barrier at the metal-semiconductor interface, which hinders fast recombination of separated charge carriers and, thus, raises their lifetime and ii) they can harvest visible light due to surface plasmon resonance (SPR) absorption.[3] So far, almost exclusively the SPR properties of Au nanoparticles (absorbing at ca. 550 nm) were investigated for photocatalytic water reduction by visible light.[3f, 4] Though the other coinage metals Ag and Cu also show SPR in the visible region, their application for photocatalytic water reduction is limited to a few examples only.[5] Moreover, Cu-based photocatalysts were mostly investigated in water reduction using UV-light containing excitation sources,[6] while the impact of SPR-active Cu particles on H_2 production under pure visible light has hardly been explored explicitly. This is also true for detailed analysis by in situ methods of the structure of the active Cu species and their formation from precursor stages under photocatalytic water reduction conditions. This, however, should provide more authentic information than ex situ studies of the catalysts before and after use and may be very helpful for rational catalyst design. Thus, we have shown by in situ EPR spectroscopy for Au/TiO_2 catalysts that SPR-promoted direct electron transfer from Au particles to TiO_2 is the initial step in visible-light driven H_2 generation[7] and that this property is sensitive to the nature of the TiO_2 support, i. e., to the content of Ti^{3+} defects and surface OH groups.[8]

In this work, we extend our studies to plasmonic monometallic Cu and mixed CuAu particles supported on TiO_2, since replacement of Au by less expensive Cu would be an economically attractive, low-cost alternative. In situ methods such as X-ray absorption near edge structure (XANES), UV-vis and Electron Paramagnetic Resonance (EPR) spectroscopy were applied in addition to Scanning Transmission Electron Microscopy (STEM) and X-ray Photoelectron Spectroscopy (XPS) to study the influence of different synthesis protocols on catalyst structure and relations between the latter and H_2 production rates under UV-vis and pure visible light, respectively.

In order to achieve an efficient photocatalytic H_2 production rate, and thereby to allow mechanistic studies in relation to specific reactivities, we used the sacrificial reductant methanol as hole scavenger, which is more easily oxidized than OH^- ions in water molecules.[9] By scavenging the positive holes in the valence band, the recombination of the photoinduced charge carriers is suppressed which leads to higher H_2 production rates.

[a] Dr. J. B. Priebe, Dr. C. Kreyenschulte, Dr. H. Junge, Prof. Dr. M. Beller, Prof. Dr. A. Brückner
Leibniz Institute for Catalysis at University of Rostock (LIKAT)
Albert-Einstein-Str. 29a, 18059 Rostock, Germany
E-mail: angelika.brueckner@catalysis.de
[b] Dr. Jörg Radnik
Federal Institute for Materials Research (BAM)
Unter den Eichen 44-46, 12203 Berlin, Germany
[c] Dr. A. J. J. Lennox
Department of Chemistry, University of Wisconsin
Madison, 1101 University Ave, Madison, WI 53706

Supporting information for this article is given via a link at the end of the document.

Results and Discussion

Photocatalytic performance

Table 1 summarizes the metal contents and H_2 production rates for all catalysts. The bare support showed only very small H_2 evolution with UV-vis light and no activity at all under visible light. Both monometallic Cu catalysts Cu-IM and Cu-RP showed similar H_2 production of 5.2 and 6.3 mmol·g^{-1}·h^{-1}, respectively, under UV-vis light (for H_2 evolution curves see Fig. S1). However, given that Cu-RP contains only 60 % of the desired Cu content, this catalyst is much more active than Cu-IM with 1.1 wt.-% Cu. This difference is even more pronounced under visible light (400−700 nm), when H_2 production is by a factor of 2.8 higher than on Cu-IM (Table 1).

Table 1. H_2 production rate, total (ICP-OES) and surface metal percentage (XPS)

Catalyst[a]	H_2 formation [mmol·g^{-1}·h^{-1}][a]		Metal content [wt. %]	
	UV-vis	vis	ICP-OES	XPS
Cu-IM	5.2	0.19	1.1	2.7
Cu-RP	6.3	0.53	0.6	2.7
Cu/Au-SP	11	0.48	0.2/0.2	3.9/0.1
Cu/Au-CP	7.5	1.6	0.2/0.2	1.2/0.1
bare P25	0.4	none	-	-
Au/P25[b]	33	2.4	0.93	0.57

[a] Conditions: 25 mg catalyst in 10 mL H_2O/MeOH (vol. ratio 1:1), 2.5 W output Hg lamp (UV-vis: 320–500 nm, vis: 400–700 nm); [b] Values taken from ref. [8]. Test conditions: 50 mg catalyst in 10 mL H_2O/MeOH (vol. ratio 1:1), 2.5 W output Hg lamp (UV-vis: 320–500 nm, vis: 400–700 nm).

In general, both bimetallic Cu/Au catalysts are more active than the monometallic Cu samples, though significant differences are observed depending whether the synthesis was performed by stepwise precipitation (Cu/Au-SP) or by coprecipitation (Cu/Au-CP). A marked improvement under UV-vis irradiation is only observed for Cu/Au-SP, while for Cu/Au-CP this is true only under visible light. In this case, the latter sample evolved more than three times the volume of H_2 as observed for Cu-RP (1.6 mmol·g^{-1}·h^{-1}, Table 1). This is remarkable, considering that our best monometallic 1% Au/P25 catalyst with twice the total metal content than Cu/Au-CP (shown for comparison in Table 1) gave only a slightly higher H_2 evolution rate of 2.4 mmol·g^{-1}·h^{-1}, yet at a lamp output of 7.5 W.[8] This illustrates that it is possible to replace noble Au partly by non-noble Cu without loss of activity. Certainly, the different activities listed in Table 1 originate from structural differences of the catalysts which are presented in the next sections.

Characterization of monometallic Cu-TiO_2 catalysts

The XRD powder patterns of all catalysts are essentially identical, showing only the anatase and rutile reflections expected for P25 (Fig. S2).

In the XP spectra, a Cu 2$p_{3/2}$ peak around 932.5 eV was detected for all samples (Table 1), which is characteristic for reduced Cu rather than for the fully oxidized Cu^{II} state.[6b, 6g] Since partial reduction of small CuO species on TiO_2 upon transfer of the catalyst into the high-vacuum XPS chamber cannot be avoided[10], the peak position is not really meaningful and, therefore, only the surface metal contents are given in Table 1. The UV-vis spectra of both monometallic Cu-IM and Cu-RP catalysts show a broad band above 600 nm, which is characteristic for *d*-*d*-transitions of Cu^{II} (Fig. 1, black line).

It has already been shown that CuO supported on TiO_2 can produce H_2 from H_2O/MeOH mixtures under UV light, due to effective charge separation within the TiO_2 support and electron transfer from the TiO_2 to the CuO conduction band, which is more positive.[11] However, the typical SPR band of Cu^0 particles at 580 nm appears immediately when catalyst Cu-RP is suspended in H_2O/MeOH in the dark and it gains intensity upon UV-vis irradiation (Fig. 1b, red and blue lines). In sample Cu-IM, this band is only formed under light irradiation and it is much weaker. This shows that light-driven in situ-formation of Cu^0 particles is much more pronounced in sample Cu-RP – an effect which is also evident from in situ XANES spectra discussed below (Fig. 2).

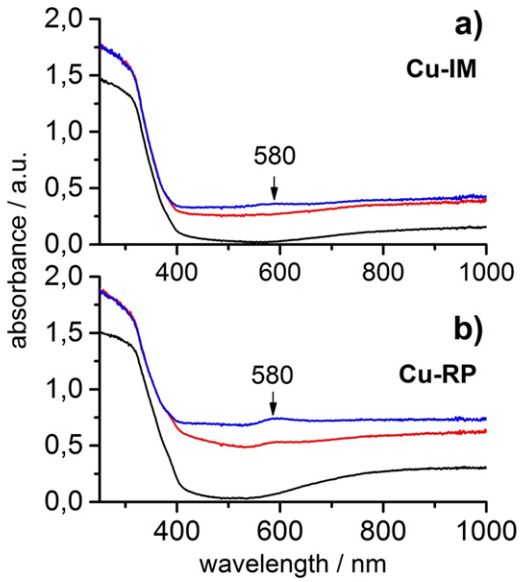

Figure 1. In situ UV-vis spectra of the monometallic Cu-based catalysts prepared by a) impregnation (Cu-IM) and b) reductive precipitation using $NaBH_4$ (Cu-RP) in the as-synthesized state (black), exposed to H_2O/MeOH in the dark (red) and under subsequent UV-vis irradiation for 5 min (blue).

While this difference has a crucial impact on H_2 evolution under visible light (Cu-RP is 2.8 times more active), it plays a minor role under irradiation with UV light (Table 1). This suggests that visible light driven H_2 formation inevitably requires the presence of plasmonic Cu^0 species while, with UV light, H_2 can also be liberated from CuO_x species as observed previously.[10] This conclusion is also supported by HR-STEM/EDX results of the as-prepared sample Cu-IM that revealed only few very small Cu-containing agglomerates while the majority of Cu is most probably highly dispersed on the support, though this could not be detected unequivocally by EDX due to the low signal-to-noise ratio (Fig. S3). In contrast, small (oxidic) CuO_x clusters of about 1-2 nm are already preformed in

as-prepared Cu-RP which, in the presence of H_2O/MeOH, might be reduced to plasmonic Cu^0 particles (Fig. S4).

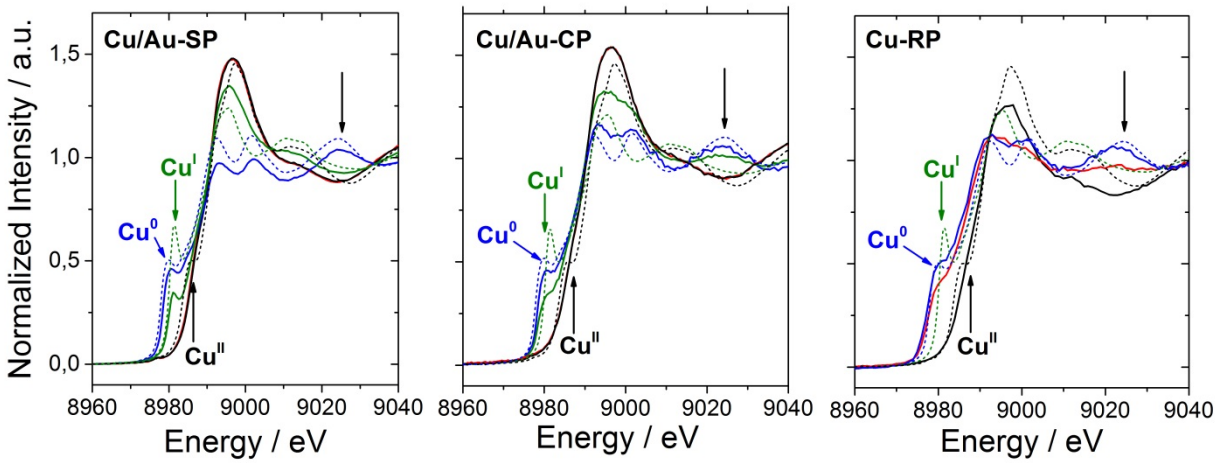

Figure 2. In situ XANES spectra of Cu-RP, Cu/Au-SP and Cu/Au-CP in the dark (black), under H_2O/MeOH in the dark (red) and under subsequent irradiation with visible (green) and UV light (blue). Dashed lines: spectra of reference materials CuO (black), Cu_2O (green) and Cu foil (blue).

In all as-prepared catalysts, the position of the absorption edge is characteristic for Cu^{II}, as evident from the superposition with the respective CuO reference. When the catalysts are exposed to the H_2O/MeOH mixture still in the dark, fast reduction of Cu^{II} to Cu^0 occurs in sample Cu-RP, while Cu in catalysts Cu/Au-SP and Cu/Au-CP remains essentially divalent. A reason may be that the higher electron affinity of Au in comparison to Cu hampers the reduction of Cu^{II} to Cu^0 in the absence of UV-vis irradiation.

Upon analyzing the catalysts under the same conditions by in situ UV-vis spectroscopy, additional information about the formation of plasmonic metal particles has been obtained (Fig. 3). The spectra of the as-synthesized samples Cu/Au-SP and Cu/Au-CP (black) contain a weak SPR absorption band of Au nanoparticles around 550-555 nm, which are probably too few to be detected by XANES. Upon suspending in H_2O/MeOH (red), no significant spectral changes were observed for sample Cu/Au-SP (Fig. 3b). In contrast, under the same conditions, a clear shift of the SPR absorption maximum from 555 to 570 nm, i. e., a position in between those of the SPR bands of pure Au and Cu (λ = 580 nm[12]), is evident for catalyst Cu/Au-CP (Fig. 3a, red). This suggests that mixed Cu-Au particles might have formed. This band still increases in intensity under irradiation but does not change its position (Fig. 3a, blue line).

Differently, SPR bands of pure Cu^0 appear under irradiation in Cu/Au-SP (Fig. 3b, blue line). Upon comparison of samples Cu/Au-SP and -CP it is readily evident that the reductive precipitation protocol has an important impact on the nature of the formed metal particles and in turn on the H_2 evolution activity (Table 1). Therefore, detailed investigations by TEM, in situ XANES and in situ EPR spectroscopy have been performed on both Cu/Au catalysts to derive structure-reactivity relationships in hydrogen generation.

HR-STEM images of sample Cu/Au-SP (Fig. 4) combined with EDX analysis (Fig. S5, S6) revealed Cu agglomerates of 1–2 nm size (Fig. 4c) separated from slightly larger Au particles (2- 5 nm, Fig. 4a) which contain traces of Cu, too. These Cu agglomerates are oxidic in the as-prepared catalyst (Fig. 2) and get reduced to plasmonic Cu^0 particles during irradiation with UV-vis light, giving rise to the SPR band at 580 nm (Fig. 3b). When Cu and Au were precipitated simultaneously in the Cu/Au-CP catalyst, well ordered mixed Cu-Au nanocrystals of 4-8 nm size are formed (Fig. 4b and d, Fig. S6). Moreover, the presence of Cu without obvious agglomeration has been detected by EDX in any support area analyzed, suggesting a more or less uniform distribution of highly dispersed Cu on the support surface. Possibly, a part of this Cu diffused into the subsurface of the support where it is not accessible by XPS anymore. This is suggested by the much smaller surface Cu content in sample Cu/Au-CP compared to Cu/Au-SP. Under ambient air, the mixed Cu-Au particles might contain copper in its oxidized form, which is reduced to Cu^0 only in the presence of H_2O/MeOH, as seen from the red-shift of the SPR absorption maximum for Cu/Au-CP (Fig. 3a, red).[13]

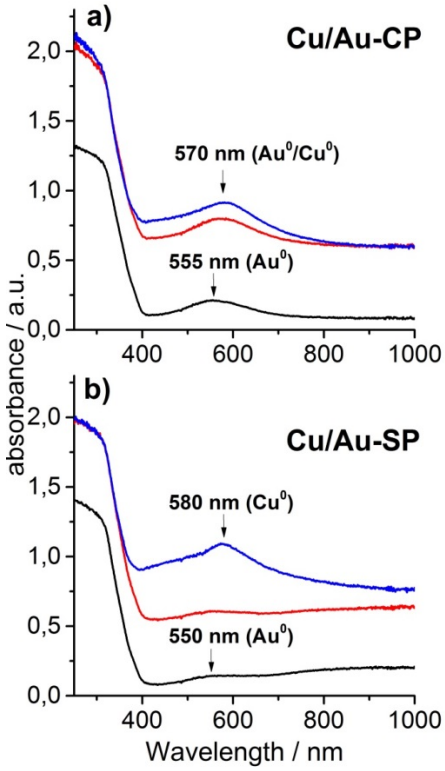

Figure 3. In situ UV-vis spectra of bimetallic catalysts, a) Cu/Au-CP and b) Cu/Au-SP as prepared in the dark (black lines), in the presence of H_2O/MeOH in the dark (red lines) and with subsequent UV-vis-light irradiation (blue lines).

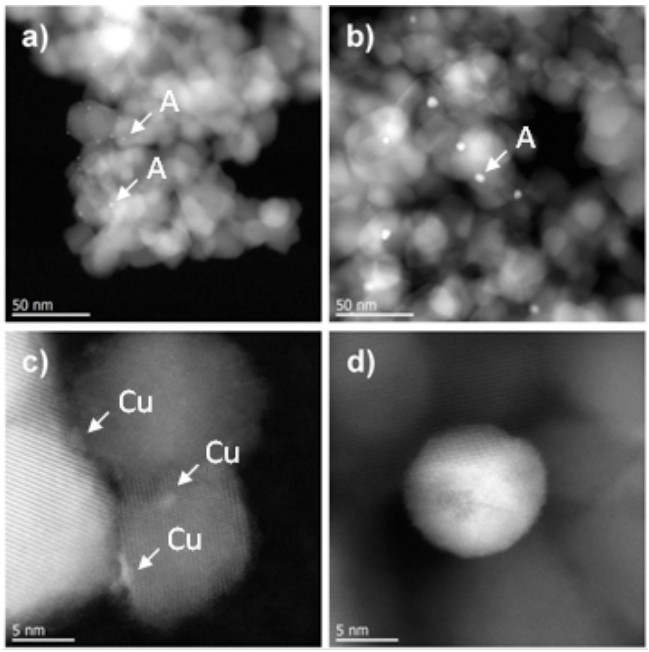

Figure 4. STEM-HAADF images of Cu/Au-SP (a, c) and Cu/Au-CP (b, d). For EDX analysis see Fig. S5 and S6.

The different mutual arrangement of Au and Cu in the bimetallic catalysts also influences the reducibility of Cu, as evident from the XANES spectra (Fig. 2). The results are compared with those obtained for the monometallic sample Cu-RP. Addition of H_2O/MeOH to this latter sample led to the reduction of Cu^{II} to Cu^0, but did not affect the position of the absorption edge in both Cu/Au catalysts (Fig. 2, red lines). With evidence from the weak SPR band in the UV-vis spectrum (Fig. 3a), the number of metallic Cu-Au particles in sample Cu/Au-CP (Fig. 3a) might be too small to be reflected by the XANES spectrum. Subsequent irradiation with visible light (green lines) caused reduction of Cu^{II}. However, while this reduction stops at Cu^{I} in sample Cu/Au-SP, metallic Cu^0 is formed under the same conditions in the Cu/Au-CP catalyst which showed much higher H_2 generation under pure visible light. The different reduction behavior of both Cu/Au catalysts can be clearly distinguished by the shape of the pre-edge feature of the absorption edge. In sample Cu/Au-SP a clear maximum is observed at 8980 eV, which is typical for Cu^{I}. In sample Cu/Au-CP this maximum is missing. Instead, the pre-edge resembles that of the Cu^0 reference. Additionally, a maximum at 9020 eV for metallic Cu can be seen in this sample, which was not found in Cu/Au-SP.

This, once again, verifies that it is the metallic plasmonic state of coinage metals that is crucial for proton reduction under visible light rather than the oxidized metal species such as Cu_2O or CuO, despite the fact that Cu_2O is known as a visible light absorber as well.[14] In contrast to the mixed Cu-Au particles in sample Cu/Au-CP, visible light alone cannot reduce oxidic Cu to its metallic state when the latter is spatially separated from Au in the Cu/Au-SP catalyst. In this case UV light is necessary to form Cu^0 (Fig. 2, blue) that then occurs as a consequence of charge separation within TiO_2 followed by electron transfer to the CuO_x species. The high dispersion of very small metal centers all over the support in Cu/Aug-SP (Fig. 4a and c) is especially beneficial for H_2 generation mediated by UV-light, since in this case TiO_2 valence-band electrons are excited and transferred to the metal particles. The smaller the metal particles, the more active sites can trap electrons and reduce protons. This is confirmed by the markedly higher H_2 rate under UV light for Cu/Au-SP (Table 1).

Besides XANES and UV-vis spectroscopy we have used in situ EPR as a third complementary method able to selectively monitor the behavior of Cu^{II} species during formation of the active catalyst from the precursor state (Fig. 5). The spectra of both samples Cu/Au-SP and Cu/Au-CP in the presence of H_2O/MeOH in the dark contain characteristic signals of Cu^{II} in axial geometry (d^9, S = 1/2). The hyperfine structure (hfs) arising from the coupling of the electron with the nuclear spin of ^{63}Cu and ^{65}Cu (I = 3/2, natural abundance 69.09 and 30.91 %, respectively) is poorly resolved, due to dipolar magnetic interaction between neighboring Cu^{II} sites, which leads do line broadening. A more detailed evaluation reveals that the spectra comprise signals from different Cu^{II} species (Fig. S7). Signal A with $g_{||} = 2.38$, $A_{||} \approx 80$ G and $g_{\perp} = 2.05$ is similar to the one previously observed from Cu^{II} located in Ti vacancies of the support surface.[15] Signal B ($g_{||}$ = 2.25, $g_{\perp}$ = 2.05, unresolved hfs) shows a more pronounced line broadening, which is due to strong dipolar interactions between Cu^{II} ions in oxidized Cu clusters.[15] This kind of Cu species dominates in the spectra of both bimetallic catalysts. Upon irradiation with visible light, the signal of Cu^{II} decreases since

these species are reduced to EPR-silent Cu^{I} and Cu^{0}. Since sample Cu/Au-SP contains almost all the copper in the form of highly dispersed Cu^{II} species, the initial signal intensity is higher and the decline is faster than in sample Cu/Au-CP in which most of the Cu forms mixed particles of larger size with Au and is therefore less dispersed. It is evident from XANES (Fig. 2) and UV-vis spectroscopy (Fig. 3) that switching to UV light causes further reduction to Cu^{0}. In sample Cu/Au-CP, this leads to a further drop of the Cu^{II} signal while, surprisingly, it increases in Cu/Au-SP despite ongoing formation of EPR-silent Cu^{0}. The reason may be that these Cu^{0} species reduce dipolar interactions between the fewer remaining Cu^{II} species, which leads to line narrowing and increase of the signal amplitude. In any case, the behavior of the Cu^{II} signal in both catalysts parallels the results of in situ XANES and in situ UV-vis measurements and reflects the facilitated reduction of Cu to the metallic state in the most active catalyst Cu/Au-CP.

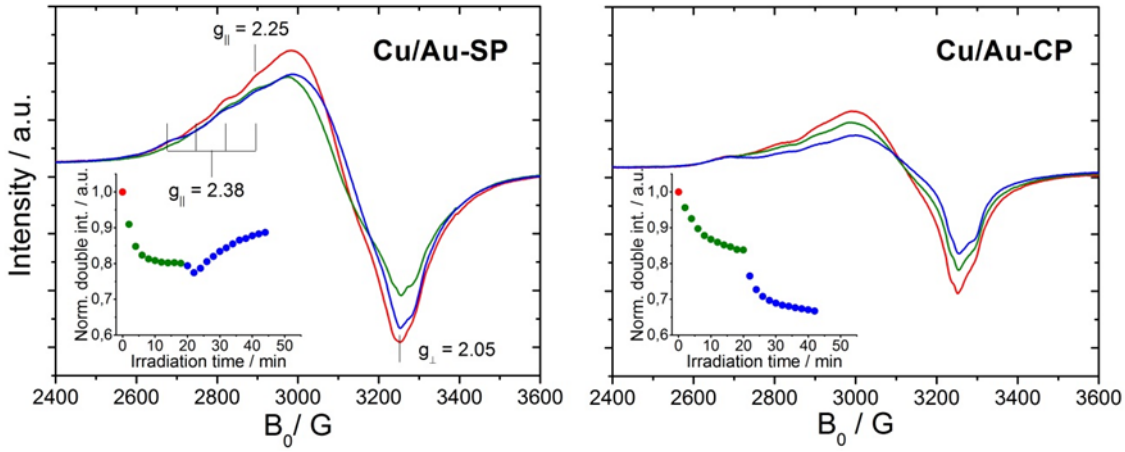

Figure 1. In situ EPR spectra of Cu/Au-SP and Cu/Au-CP under H_2O/MeOH in the dark (red) and subsequent visible- (green) and UV-light irradiation (blue). Insets: signal intensity as a function of irradiation time.

Conclusions

H_2 production from H_2O/MeOH mixtures by monometallic Cu-TiO_2, as well as bimetallic Cu/Au-TiO_2 catalysts depends crucially on the nature of the metal particles which itself is governed by the synthesis procedure. Thus, Cu species deposited on TiO_2 by reductive precipitation (Cu-RP) are easily reduced in situ to plasmonic Cu^{0} particles under photocatalytic conditions, while this is much more difficult for a catalyst prepared by impregnation (Cu-IM), in which no clear metal particles but highly dispersed Cu species are formed. This leads to an almost threefold H_2 production rate of Cu-RP under pure visible light (despite an only half as high metal content as in Cu-IM). This shows clearly that it is the plasmonic Cu^{0} particles that boost visible-light activity.

The mixed Cu/Au-SP catalyst prepared by sequential reductive precipitation of 1) Cu and 2) Au did not improve H_2 production under visible light in comparison to Cu-RP, since both metal components are separately present, whereby Cu is more highly dispersed on the support surface than Au (reflected by the XPS surface ratios). This Cu dispersion is highest in sample Cu/Au-SP, which leads to a doubling of the UV-light-driven H_2 production rate compared to Cu-RP. This is due to the different mechanism which implies charge separation within TiO_2 followed by electron trapping at surface Au and Cu sites, the latter being most abundant in catalyst Cu/Au-SP.

When Cu and Au are deposited on TiO_2 simultaneously by reductive co-precipitation (Cu/Au-CP), mixed plasmonic Cu-Au particles of 4-8 nm size are formed, which boost the H_2 production rate under visible light by a factor of almost 3, compared to the monometallic Cu-RP counterpart, despite the fact that the total metal content in Cu/Au-CP is lower by one third. Obviously, the tight mixing of Cu and Au in the oxidic precursor species raises the reduction potential of Cu and facilitates reduction to plasmonic metal particles that are essential for visible-light-driven H_2 generation. Remarkably, visible-light driven H_2 production with this catalyst is almost as active as our most active monometallic 1% Au/P25 catalyst,[8] despite the lower total metal content of only 0.4 % and the lower lamp output used in the present work. This opens new opportunities to replace noble Au by less expensive Cu in such photocatalysts without loss in activity.

Experimental Section

Catalyst Preparation

All catalysts were prepared using P25 (Evonik, BET surface area: 50 m^2/g) as TiO_2 support, which consists of 85 % anatase and 15 % rutile. Monometallic Cu/TiO_2 was prepared by two different procedures. *a) Impregnation* was carried out by suspending 1.0 g TiO_2 powder in 300 mL absolute alcohol. An aqueous solution of $Cu(NO_3)_2 \cdot 3H_2O$ (0.15 mm, 25 mL, Aldrich) was added dropwise. The mixture was stirred for 10 h at 80 °C,

filtered and washed with 500 mL distilled water. After drying at 100 °C for 12 h, the material was calcined at 500 °C (3 K/min) for 3 h in flowing air. The catalyst is denoted by Cu-IM. *b) Reductive precipitation* was carried out by suspending 1.0 g TiO_2 in 20 mL H_2O. After adding an aqueous solution of $Cu(NO_3)_2{\cdot}3H_2O$ (0.15 mm, 5 mL, Aldrich), a freshly prepared solution of $NaBH_4$ (0.1 m, 4 mL) was dropped into the suspension. The mixture was stirred for 20 min and the catalyst was filtered, washed, dried at 100 °C for 12 h and denoted by Cu-RP. Mixed Cu/Au metal catalysts were also prepared via the reductive precipitation method, though with different reaction sequences. *c) Stepwise precipitation* (denoted by -SP) was carried out by first dropping an aqueous $NaBH_4$ solution (0.1 m, 4 mL) into 20 mL of an aqueous suspension containing 1 g TiO_2 and 36 mg $Cu(NO_3)_2{\cdot}3H_2O$. After 20 min, 4.0 mg $HAuCl_4{\cdot}3H_2O$ (Aldrich) in 10 mL H_2O were added dropwise followed by subsequent addition of further $NaBH_4$ solution (0.1 m, 1 mL). After stirring for 10 min, the material was filtered, washed and dried at 100 °C for 12 h. *d) Co-precipitation* was applied to prepare a mixed Cu,Au/TiO_2 catalyst by adding an aqueous $NaBH_4$ solution (0.1 m, 5 mL) to 50 mL of an aqueous suspension containing 1 g TiO_2, 36 mg $CuNO_3{\cdot}3H_2O$ and 4.0 mg $HAuCl_4{\cdot}3\ H_2O$. The mixture was stirred for 30 min, filtered, washed and dried for 12 h at 100 °C (denotation: Cu/Au-CP).

Photocatalytic tests

Photocatalytic tests were carried out at 25 °C under argon atmosphere with freshly distilled solvents using 25 mg catalyst in 10 mL MeOH/H_2O (vol. ratio: 1/1) and a 2.5 W Hg vapor light irradiation source (Lumatec Superlite 400). Further details on the equipment and the experimental set-up have been published previously.[16] The gas evolution was recorded first under visible light (400−700 nm filter) for ca. 6 h and subsequently under UV-vis light (320−500 nm filter) for ca. 2.5 h. After each reaction, a gas sample was taken for gas chromatography in order to determine the relative composition of the evolved gases (GC HP 6890N, carboxen 1000, TCD, external calibration). The variation of the hydrogen volumes for repeat experiments is between 5−25 %, including the error of the measurement set-up itself as well as the reproducibility of the catalyst preparation method.

Catalyst characterization

UV-vis spectra in reflectance mode were recorded by an Avantes AvaSpec-2048 UV-vis spectrometer with a 45 ° optical probe from catalysts in pure form and suspended in H_2O/MeOH (1 : 1) before and during irradiation with UV-vis light (same irradiation source as used for catalytic tests). The amount of deposited metals was determined by ICP-OES using a Varian 715-ES ICP-emission spectrometer and the ICP Expert software. XRD powder patterns were recorded in transmission mode with Cu Kα radiation in the 2θ range of 10-70° (step width = 0.25°) on a Stoe STADI P diffractometer, equipped with a linear position sensitive detector.

In situ EPR spectra in X-band were recorded at room temperature by a Bruker EMX CW-microspectrometer in “home-made” flow cells while passing a helium carrier-gas stream (30 mL/min) saturated with 5 % water and methanol (1 : 1) through the catalyst. An ER 4119HS-WI high-sensitivity optical resonator with a grid in the front side enabled irradiation of the samples with a 300 W Xe-arc lamp (LOT Oriel) equipped with an optical cut-off filter (LOT Oriel GG420). *g* values were calculated using the equation $h\nu = g\beta B_0$ with B_0 and ν being the resonance field and frequency, respectively. *g* values were calibrated using a DPPH standard (g = 2.0036 ± 0.00004).

In situ XANES experiments were conducted at the µ-spot beamline of the synchrotron storage ring BESSY in Berlin (Germany) at the Cu K edge in fluorescence mode with a 7-element Si(Li) array detector. All samples were filled in quartz glass capillaries with a diameter of 2 mm and a wall thickness of 0.01 mm. After taking the spectrum of the pure solid, a 1:1 mixture of water and methanol was added. These suspensions were irradiated using the same lamp as for the in situ EPR measurements. As references Cu foil, Cu_2O and CuO were used. The XANES spectra were normalized in the pre-edge range between 8890 and 8950 eV with a linear and in the post-edge range between 9010 and 9100 eV with a cubic function as background.

TEM investigations were performed at 200 kV by a JEM-ARM200F (JEOL) instrument equipped with a JED-2300 (JEOL) energy-dispersive X-ray spectrometer (EDXS) for chemical analysis. EDX spectra and high-angle annular dark field (HAADF) images were acquired with a spot size of 5c (ca. 0.15 nm) and a 30 µm condenser aperture. Prior to TEM analysis, the dry sample was deposited on a carbon-supported Ni grid.

XP spectra were recorded using a VG ESCALAB 220iXL instrument with Al K_α radiation (E = 1486.6 eV). Peaks were fitted by Gaussian–Lorentzian curves after Shirley background subtraction. The electron binding energy was referenced to the Ti $2p_{3/2}$ peak of TiO_2 at 458.8 eV. For quantitative analysis, the peak areas were determined and divided by the element-specific Scofield factor and the analysator-depending transmission function.

Acknowledgements

Financial support by Deutsche Forschungsgemeinschaft (DFG – SPP1613) and the Alexander von Humboldt foundation is gratefully acknowledged. For their help with XANES measurements we thank U. Reinholz, M. Radtke and F. Emmerling (Federal Institute of Material Research and Testing, Berlin). We thank BESSY II (Helmholtz-Zentrum Berlin) for technical assistance.

Keywords: photocatalysis • in situ spectroscopy • surface plasmon resonance • hydrogen generation • bimetallic catalysts

[1] a) A. Kudo, Y. Miseki, *Chem. Soc. Rev.* **2009**, *38*, 253-278; b) A. Fujishima, *Nature* **1972**, *238*, 37-38; c) N. Armaroli, V. Balzani, *Angew. Chem. Int. Edit.* **2007**, *46*, 52-66.

[2] M. R. Hoffmann, S. T. Martin, W. Choi, D. W. Bahnemann, *Chem. Rev.* **1995**, *95*, 69-96.

[3] a) D. B. Ingram, S. Linic, *J. Am. Chem. Soc.* **2011**, *133*, 5202-5205; b) S. Linic, P. Christopher, D. B. Ingram, *Nat. Mater.* **2011**, *10*, 911-921; c) P. Christopher, D. B. Ingram, S. Linic, *J. Phys. Chem. C* **2010**, *114*, 9173-9177; d) S. K. Cushing, J. Li, F. Meng, T. R. Senty, S. Suri, M. Zhi, M. Li, A. D. Bristow, N. Wu, *J. Am. Chem. Soc.* **2012**, *134*, 15033-15041; e) A. Primo, A. Corma, H. García, *Phys. Chem. Chem. Phys.* **2011**, *13*, 886-910; f) C. Gomes Silva, R. Juárez, T. Marino, R. Molinari, H. García, *J. Am. Chem. Soc.* **2011**, *133*, 595-602; g) H. Y. Lin, Y. S. Chang, *Int. J. Hydrogen Energ.* **2010**, *35*, 8463-8471; h) K. Ueno, T. Oshikiri, H. Misawa, *ChemPhysChem* **2016**, *17*, 199-215; i) P. Zhang, T. D. Wang, J. Gong, *Adv. Mater.* **2015**, *27*, 5328-5342.

[4] a) Z. Liu, W. Hou, P. Pavaskar, M. Aykol, S. B. Cronin, *Nano Lett.* **2011**; b) E. Thimsen, F. Le Formal, M. Grätzel, S. C. Warren, *Nano Lett.* **2011**; c) S. C. Warren, E. Thimsen, *Energ. Environ. Sci.* **2012**, *5*, 5133-5146; d) J. J. Chen, J. C. S. Wu, P. C. Wu, D. P. Tsai, *J. Phys. Chem. C* **2011**; e) A. Primo, T. Marino, A. Corma, R. Molinari, H. García, *J. Am. Chem. Soc.* **2011**; f) J. Lee, S. Mubeen, X. Ji, G. D. Stucky, M. Moskovits, *Nano Lett.* **2012**, *12*, 5014-5019; g) I. Thomann, B. Pinaud, Z. Chen, B. Clemens, T. Jaramilo, M. L. Brongersma, *Nano Lett.* **2011**; h) S. S. Rayalu, D. Jose, M. V. Joshi, P. A. Mangrulkar, K. Shrestha, K. Klabunde, *Appl. Catal. B: Environ.* **2013**, *142*, 684-693.

[5] a) M. Z. Ge, C. Y. Cao, S. H. Li, Y. X. Tang, L. N. Wang, N. Qi, J. Y. Huang, K. Q. Zhang, S. S. Al-Deyab, Y. K. Lai, *Nanoscale* **2016**, *8*, 5226-5234; b) J. M. Kum, Y. J. Park, H. J. Kim, S. O. Cho, *Nanotechnology* **2015**, *26*; c) Z. Lian, W. Wang, S. Xiao, X. Li, Y. Cui, D. Zhang, G. Li, H. Li, *Scientific Reports* **2015**, *5*; d) H. Liu, T. Wang, H. Zeng, *Part. Part. Syst. Charact.* **2015**, *32*, 869-873; e) L. Sinatra, A. P. Lagrow, W. Peng, A. R. Kirmani, A. Amassian, H. Idriss, O. M. Bakr, *J. Catal.* **2015**, *322*, 109-117.

[6] a) N.-L. Wu, M.-S. Lee, *Int. J. Hydrogen Energ.* **2004**, *29*, 1601-1605; b) Y. Wu, G. Lu, S. Li, *Catal. Lett.* **2009**, *133*, 97-105; c) S. Xu, J. Ng, X. Zhang, H. Bai, D. D. Sun, *Int. J. Hydrogen Energ.* **2010**, *35*, 5254-5261; dJ. Yu, J. Ran, *Energ. Environ. Sci.* **2011**, *4*, 1364-1371; e) V. Gombac,

L. Sordelli, T. Montini, J. J. Delgado, A. Adamski, G. Adami, M. Cargnello, S. Bernal, P. Fornasiero, *J. Phys. Chem. A* **2009**, *114*, 3916-3925; f) T. Montini, V. Gombac, L. Sordelli, J. J. Delgado, X. Chen, G. Adami, P. Fornasiero, *ChemCatChem* **2011**, *3*, 574-577; g) H.-J. Choi, M. Kang, *Int. J. Hydrogen Energ.* **2007**, *32*, 3841-3848; hP. Gomathisankar, K. Hachisuka, H. Katsumata, T. Suzuki, K. Funasaka, S. Kaneco, *Int. J. Hydrogen Energ.* **2013**, *38*, 11840-11846.

[7] J. B. Priebe, M. Karnahl, H. Junge, M. Beller, D. Hollmann, A. Brückner, *Angew. Chem. Int. Ed.* **2013**, *52*, 11420-11424.

[8] J. B. Priebe, J. Radnik, A. J. J. Lennox, M. M. Pohl, M. Karnahl, D. Hollmann, K. Grabow, U. Bentrup, H. Junge, M. Beller, A. Brückner, *ACS Catal.* **2015**, *5*, 2137-2148.

[9] M. Ni, M. K. H. Leung, D. Y. C. Leung, K. Sumathy, *Renew. Sust. Energ. Rev.* **2007**, *11*, 401-425.

[10] H. Irie, K. Kamiya, T. Shibanuma, S. Miura, D. A. Tryk, T. Yokoyama, K. Hashimoto, *J. Phys. Chem. C* **2009**, *113*, 10761-10766.

[11] J. Bandara, C. Udawatta, C. Rajapakse, *Photochem. Photobiol. Sci.* **2005**, *4*, 857-861.

[12] X. Guo, C. Hao, G. Jin, H. Y. Zhu, X. Y. Guo, *Angew. Chem. Int. Ed.* **2014**, *53*, 1973-1977.

[13] C. L. Bracey, P. R. Ellis, G. J. Hutchings, *Chem. Soc. Rev.* **2009**, *38*, 2231-2243.

[14] W. Y. Cheng, T. H. Yu, K. J. Chao, S. Y. Lu, *ChemCatChem* **2014**, *6*, 293-300.

[15] G. Li, N. M. Dimitrijevic, L. Chen, T. Rajh, K. A. Gray, *J. Phys. Chem. C* **2008**, *112*, 19040-19044.

[16] F. Gärtner, S. Losse, A. Boddien, M. M. Pohl, S. Denurra, H. Junge, M. Beller, *ChemSusChem* **2012**, *5*, 530-533.

Entry for the Table of Contents

All that glitters isn´t gold. The impact of different metal deposition methods on light-driven H_2 production is studied. Au/Cu alloy particles formed by coprecipitation evolve much more H_2 under vis light than separate Au^0 and Cu^0 particles formed by stepwise precipitation. The opposite is true under UV light.